A GLP-Compliant Toxicology and Biodistribution Study: Systemic Delivery of an rAAV9 Vector for the Treatment of Mucopolysaccharidosis IIIB

Aaron S. Meadows,[1] F. Jason Duncan,[1] Marybeth Camboni,[1] Kathryn Waligura,[1] Chrystal Montgomery,[1] Kimberly Zaraspe,[1] Bartholomew J. Naughton,[1] William G. Bremer,[2] Christopher Shilling,[3] Christopher M. Walker,[2,4] Brad Bolon,[5] Kevin M. Flanigan,[1,4] Kim L. McBride,[4,6] Douglas M. McCarty,[1,4] and Haiyan Fu[1,3,*]

[1]Center for Gene Therapy, [2]Center for Vaccines and Immunity, [3]Drug and Device Development Service, The Research Institute at Nationwide Children's Hospital, Columbus, Ohio; [4]Department of Pediatrics, College of Medicine and Public Health, Columbus, Ohio; [5]Comparative Pathology and Mouse Phenotyping Shared Resource, Comprehensive Cancer Center, The Ohio State University, Columbus, Ohio; [6]Center for Cardiovascular and Pulmonary Research, Columbus, Ohio.

No treatment is currently available for mucopolysaccharidosis (MPS) IIIB, a neuropathic lysosomal storage disease due to defect in α-*N*-acetylglucosaminidase (*NAGLU*). In preparation for a clinical trial, we performed an IND-enabling GLP-toxicology study to assess systemic rAAV9-CMV-h*NAGLU* gene delivery in WT C57BL/6 mice at 1×10^{14} vg/kg and 2×10^{14} vg/kg (n = 30/group, M:F = 1:1), and non-GLP testing in MPS IIIB mice at 2×10^{14} vg/kg. Importantly, no adverse clinical signs or chronic toxicity were observed through the 6 month study duration. The rAAV9-mediated rNAGLU expression was rapid and persistent in virtually all tested CNS and somatic tissues. However, acute liver toxicity occurred in 33% (5/15) WT males in the 2×10^{14} vg/kg cohort, which was dose-dependent, sex-associated, and genotype-specific, likely due to hepatic rNAGLU overexpression. Interestingly, a significant dose response was observed only in the brain and spinal cord, whereas in the liver at 24 weeks postinfection (pi), NAGLU activity was reduced to endogenous levels in the high dose cohort but remained at supranormal levels in the low dose group. The possibility of rAAV9 germline transmission appears to be minimal. The vector delivery resulted in transient T-cell responses and characteristic acute antibody responses to both AAV9 and rNAGLU in all rAAV9-treated animals, with no detectable impacts on tissue transgene expression. This study demonstrates a generally safe and effective profile, and may have identified the upper dosing limit of rAAV9-CMV-h*NAGLU* via systemic delivery for the treatment of MPS IIIB.

INTRODUCTION

Mucopolysaccharidosis (MPS) IIIB is a rare monogenic lysosomal storage disease (LSD) caused by mutations in the gene coding for α-*N*-acetylglucosaminidase (NAGLU).[1] The lack of NAGLU activity disrupts the stepwise degradation of heparan sulfate glycosaminoglycans (GAG), leading to the accumulation of nondegraded or partially degraded heparan sulfate oligosaccharides in lysosomes in cells of virtually all organs. Cells throughout the central nervous system (CNS), including neuronal and non-neuronal cells, are particularly affected, resulting in complex secondary neuropathology.[2–10] Infants with MPS IIIB appear normal at birth, but develop severe progressive neurological disorders, leading to high morbidity and premature death.[1,11,12] Somatic manifestations occur in all MPS IIIB patients, and involve virtually all organs, though they are mild relative to other forms of MPS, such as MPS I, II, and VII.

No specific treatment is currently available for MPS IIIB, and therapies have been limited to treatment of symptoms.[13] The biggest challenge in therapeutic development has been the effect of the blood brain barrier (BBB) that precludes effective agent delivery to the CNS to treat the global neuropathology of the disease.[14]

Gene therapy shows promise for LSDs because of the bystander effect of secreted lysosomal enzymes, including NAGLU, which reduces the

*Correspondence: Haiyan Fu, The Center for Gene Therapy, The Research Institute at Nationwide Children's Hospital, 700 Children's Drive, Columbus, OH 43205. E-mail: haiyan.fu@nationwidechildrens.org

DOI: 10.1089/humc.2015.132

demand for efficient gene transfer.[1,15] The adeno-associated virus (AAV) vector system offers an invaluable gene delivery tool for treating a variety of diseases, with a broad tissue tropism and absence of known pathogenesis in humans.[16] Recombinant AAV (rAAV) vectors based on AAV serotype 2 (AAV2) have been shown to transduce both neuronal and non-neuronal cells in the CNS in numerous gene therapy studies, with demonstrated therapeutic benefits in treating neurological diseases,[17] including MPS and other LSDs, in animal models.[15,18–29] Approaches using rAAV vectors have been tested in multiple phase I/II gene therapy clinical trials in patients with various neurological disorders.[30–36]

The development of novel AAV serotypes, particularly the trans-BBB neurotropic AAV serotype 9 (AAV9),[37–39] has provided efficient tools for CNS gene delivery to treat neurological diseases like MPS IIIB that have both CNS and broad somatic manifestations.[22,40,41] Previously, we treated adult MPS IIIB mice with a single systemic rAAV9 vector injection and successfully achieved permanent restoration of NAGLU activity in the CNS, peripheral nervous system (PNS), and broad somatic tissues, leading to functional correction of neurological disorders and normalized survival.[22] We also tested our systemic rAAV9-h*NAGLU* gene delivery approach in nonhuman primates at the designated minimal efficacious clinical dose (MECD), demonstrating a safe and effective profile.[42] These results strongly support the translation of this approach to the treatment of MPS IIIB in patients.

In preparation for a phase I/II clinical trial, we performed an IND-enabling GLP-toxicology/biodistribution study with dose-escalation in WT C57BL/6 mice by an intravenous (IV) injection of rAAV9-CMV-h*NAGLU* vector to further assess the safety and feasibility of the approach for clinical application in humans. At 1×10^{14} vg/kg and 2×10^{14} vg/kg, the treatment did not lead to detectable adverse clinical signs or chronic toxicity. However, we observed a dose-dependent, sex-associated, and genotype-specific acute severe liver toxicity at a very high dose (2×10^{14} vg/kg) only in WT animals, which may be very close to the upper dosing limit of the approach. These data support the clinical potential of this gene therapy approach and provide a safe path forward.

MATERIALS AND METHODS

Animals

For the GLP study, wild-type (WT) C57BL/6 mice were provided by Charles River Laboratory (CRL) and transported to CRL Preclinical Services for testing, in accordance with the applicable GLP regulations.

An MPS IIIB knock-out mouse colony[6] was maintained on an inbred background (C57BL/6) of backcrosses of heterozygotes in the Vivarium at Nationwide Children's Hospital Research Institute (NCH-RI). The genotypes of progeny mice were identified by PCR, using primers of murine *NAGLU* Exon 6 (Forward: 5′- TGGACCTGTTTGCTGAAA GC; Reverse: 5′- CAGGCCATCAA ATCT GGTAC), and neomycin (5′- TGGGATCGGCCATTGAACAA; 5′- CCTTGAGC CT GGCGAACAGT). MPS IIIB mice and their age-matched WT littermates were used in the expanded acute toxicology experiments mimicking the GLP condition.

All animal care and procedures were performed strictly following the approved protocol, in accordance with the Guide for the Care and Use of Laboratory Animals [8th Edition, 2011].

Recombinant AAV9 viral vectors

A previously described recombinant AAV9 (rAAV) vector plasmid[22] was used to produce conventional single-strand rAAV9-CMV-h*NAGLU* viral vector. The vector genomes contained minimal elements required for transgene expression, including AAV2 terminal repeats, a human cytomegalovirus (CMV) immediate-early promoter, SV40 splice donor/acceptor signal, a human *NAGLU* (h*NAGLU*) coding sequence, and BGH polyadenylation signal. The rAAV9 viral vectors were produced by SAB Tech Inc. in HEK293 cells using three-plasmid transient transfection, and purified by banding on a CsCl step gradient followed by dialysis into Tris-buffered saline (TBS, pH8.0). The purified viral vector was titrated using PAGE gel silver staining and confirmed by dot blotting. The viral vector preps were then further tested by the NCH Viral Vector Core-Clinical Manufacturing Facility (NCH-CMF) and WuXi-Apptec and released by NCH-CMF.

The transient transfection approach will also be used to produce the clinical-grade vector for a proposed phase I/II clinical trial in patients with MPS IIIB.

Toxicology and biodistribution study design

The GLP-toxicology study was performed by Charles River Laboratories (CRL) Preclinical Services in accordance with the U.S. Department of Health and Human Services, Food and Drug Administration, United States Code of Federal Regulations, Title 21, Part 58: Good Laboratory Practice for Nonclinical Laboratory Studies, with the exception of vector characterization and test-

ing, and analyses for transgene expression, biodistribution, and immune responses. This study included three cohorts (n = 30/group, M:F = 1:1) as shown in Supplementary Table S1. The animals were given an IV injection of saline (Group 1), or rAAV9-CMV-h*NAGLU* vector at 1×10^{14} vg/kg (Group 2) or 2×10^{14} vg/kg (Group 3). The animals were then observed for clinical signs, clinical grades, body weights, body weight changes, and food consumption. Necropsies were performed at 6 weeks, 12 weeks, and 24 weeks pi. Blood samples were assayed for hematology, and clinical chemistry, and antibody analysis. Tissues were analyzed for, gross necropsy findings, organ weights, transgene expression, biodistribution, T-cell response, and histopathology examination.

A 6-week, non-GLP toxicology study mimicking the GLP conditions was performed in young MPS IIIB mice and their WT littermates, all males. The animals were given an IV injection of 2×10^{14} vg/kg rAAV9-CMV-h*NAGLU* vector from the same manufacturing lot as used in the GLP study. Necropsies and tissue analyses were performed on Day 5 (D5) and 6 weeks pi.

Intravenous (IV) vector delivery

The experimental mice were treated by an IV injection of either 1×10^{14} vg/kg (Group 2) or 2×10^{14} vg/kg (Group 3) of rAAV9-CMV-h*NAGLU* vector (200μl, diluted in saline) or saline alone (Group 1) via tail vein.

Post-treatment monitoring

After injection, daily cage-side observations were performed for well-being and behavior throughout the duration of the study. Each animal was weighed at least weekly and food consumption measured quantitatively.

Assessment of clinical grades were performed 24 hr pi and on the day of necropsy, for skin condition, spontaneous activity, gate, and tail elevation during forward motion. Detailed clinical observations were performed weekly for signs of adverse effects, throughout the 24-week study duration.

Clinical pathology analyses

Blood draws were performed via submandibular vein 2 weeks prior to necropsy or via vena cava at necropsy under isoflurane anesthesia. Blood samples were examined for hematology and blood chemistry by CRL Clinical Pathology Laboratory.

The subjects were terminated at 6 weeks, 12 weeks, or 24 weeks pi. The veterinary staff euthanized the subjects by an IV injection of pentobarbital (50 mg/kg). Cerebrospinal fluid (CSF) was collected by lumbar puncture. Brain, spinal cord, dorsal root ganglion, and multiple somatic tissues (liver, kidney, spleen, heart, lung, intestines, stomach, pancreas, skeletal muscles, testis, lymph nodes) were harvested either on dry ice and stored at –80°C, or in 4% paraformaldehyde at 4°C. Each brain was divided into two hemispheres along the midline and then into multiple coronal slabs. Each slab from one sphere was further divided into matrices with 12–14 sections and each section was harvested on dry ice and stored at –80°C. Brain slabs from another sphere were stored in 4% paraformaldehyde for immunofluorescence (IF) assays and hematoxylin and eosin (H&E) staining.

Histopathology

All collected tissues were processed to produce paraffin sections (4 μm) and then stained with H&E at CRL testing facility. Histopathology evaluation was performed by a board-certified veterinary pathologist at CRL.

ELISA for antibody responses to rAAV9 vector and rNAGLU

Serum samples from the study subjects were assayed by binding ELISA for antibodies to AAV9 or rNAGLU, using purified rAAV9 vector or full-length hNAGLU protein as antigens (ag). Briefly, 1×10^{10} vg/ml of rAAV9 vector, or 20 μg/ml of full-length recombinant hNAGLU protein (custom manufactured by GenScript), in carbonate coating buffer was applied to 96-well plates and incubated over night at 4°C. The plate was then washed and blocked for 1 hr with blocking buffer (5% milk in PBS containing 0.1% Tween-20). Serial dilution of serum samples in blocking buffer were added to the plates and incubated at room temperature for 1 hr. The plates were washed with PBS-T and then incubated with horseradish peroxidase conjugated anti-mouse IgG (Sigma-Aldrich) for 1 hr at room temperature. After being washed with PBS-T, the plates were then developed with 3,3′,5,5′-tetramethylbenzidine (TMB) at RT for 5 min. The reaction was stopped by adding 1N sulfuric acid. The absorbance was read at 450 nm on a plate reader. Data were analyzed as follows: $(OD_{450}\text{-}ag^{+} - OD_{450}\text{-}ag^{-})/OD_{450}\text{-}ag^{-}$. Values ≥2 were considered to be antibody positive.

Interferon-γ enzyme-linked immunospot (ELISPOT) assay

Spleen samples were processed for T-cell responses to AAV9 and hNAGLU by interferon-γ (IFN-γ) ELISPOT assay, following previously published procedures.[43] Briefly, 10^6 splenocytes

isolated on Ficoll-Hypaque gradients were cultured with synthetic overlapping peptides (18 amino acids each in length, overlapping by 11 residues) covering the full-length AAV9 capsid protein or human NAGLU protein (custom synthesized by Ohio Peptide LLC). Each peptide was dissolved in dimethyl sulfoxide (DMSO). Peptides of each protein were organized into three pools, each containing 1 μg/peptide/ml in the culture. After incubation at 37°C for 36 hr, the plates were developed according to the manufacturer's instruction, and the IFN-γ spot-forming cells (SFC) were counted. DMSO was used as negative control and concanavalin A (ConA) was used as positive control. Fewer than 10 SFC/well were observed from negative control (DMSO). Responses were considered positive when SFC exceeded 50 per 10^6 PBMC in duplicate wells.

NAGLU activity assay

Tissue samples were assayed for NAGLU enzyme activity following a published procedure with minor modifications.[44] The assay measures 4-methylumbelliferone (4MU), a fluorescent product formed by hydrolysis of the substrate 4-methylumbellireyl-N-acetyl-α-D-glucosaminide. Tissue NAGLU activity is expressed as unit/mg protein, and 1 unit is equal to 1 nmol of 4MU released/hr at 37°C.

Immunofluorescence (IF)

Tissues were processed to obtain paraffin sections (4 μm). The tissue sections were then assayed by IF to identify cells expressing rNaGlu, using antibodies against hNAGLU (a kind gift from Dr. EF Neufeld, UCLA), and a secondary antibody conjugated with AlexaFluor^{568} (Millipore), following procedures recommended by the manufacturers. The sections were visualized under a fluorescence microscope.

Quantitative real time PCR (qPCR)

Total DNA was isolated from tissue samples of all animals using Qiagen DNeasy columns and analyzed by qPCR, using Absolute Blue QPCR Mix (Thermo Scientific) and Applied Biosystems 7000 Real-Time PCR System, following the procedures recommended by the manufacturer. Taqman primers specific for the CMV promoter were used to detect rAAV vector genomes—forward: GGCAGTA CATCAAGTGTATC; reverse: ACCAATGGTAATA GCGATG AC; probe: [6~FAM]AATGACGGTAAA TGG CCCGC[TAMRA ~6~FAM]. Genomic DNA was quantified in parallel samples using murine β-actin-specific primers—forward: CCTTCCGTCC TCAGATCATT; reverse: CTTGCTGATCCACAT CTGCT; probe: [6~FAM] CATCCTGGCCTCGCT GC CA[Tamra~Q]. Genomic DNA from non-treated mouse tissues was used as controls for background levels and absence of contamination. Tissues from mice in the GLP study were assayed by CRL. Tissues from mice in the non-GLP study were assayed by our laboratory.

Statistical analyses

Means, standard deviation (SD), and Student *t*-test were used for quantitative data analyses. The significance level was set at $P \leq 0.05$.

RESULTS

Findings from the GLP-compliant toxicology and biodistribution testing in WT C57BL/6 mice

In preparation for a phase I/II clinical trial, we performed an IND-enabling GLP-toxicology/biodistribution study to assess safety and feasibility of systemic rAAV9-CMV-h*NAGLU* gene delivery in WT C57BL/6 mice (Supplementary Table S1), following FDA guidelines. The mice were randomized into three cohorts (n = 30/group, M:F = 1:1), receiving an IV injection of saline (Group 1), or rAAV9-CMV-h*NAGLU* at 1×10^{14} vg/kg or 2×10^{14} vg/kg respectively. Animals were observed twice daily and clinical grade assessed weekly throughout the study for general health signs of illness, toxicity, unusual or abnormal appearance, body weight (BW), and morbidity. Necropsies were performed at 6 weeks, 12 weeks, and 24 weeks pi for tissue analyses (n = 8–10/group, M:F = 1:1), to assess the acute, intermediate and chronic toxicology, biodistribution, and transgene expression.

Dose-dependent and sex-specific severe acute liver toxicity in WT C57BL/6 mice. In the GLP Toxicology study, an IV injection of 2×10^{14} vg/kg rAAV9-CMV-h*NAGLU* led to sudden acute mortality in 5 of 15 male mice, including 3 mice on Day (D) 6 and 2 mice on D8 pi. No adverse clinical signs were noted preceding the deaths. All five animals exhibited liver pallor that correlated microscopically with severe hepatic necrosis and vacuolation, without detectable leukocyte infiltration. Immunofluorecence for hNAGLU showed high levels of rNAGLU in necrotic hepatocytes in postmortem liver tissue samples from these mice (Supplementary Fig. S1). Importantly, there were no vector-related deaths throughout the rest of the study duration between D9 and 24 weeks pi. These data suggest that an IV injection of rAAV9-CMV-h*NAGLU* led to a dose-dependent and sex-associated acute liver toxic-

ity due to rNAGLU overexpression rather than inflammatory involvement.

Systemic delivery of rAAV9-CMV-hNAGLU vector did not lead to observable clinical signs. No vector treatment-related clinical signs were observed over the entire 6-month duration of this study, even in the five male mice that died on D6 and D8 postinjection.

In both rAAV9-treated cohorts, significant BW losses were noted within 1 week pi, compared to nontreated controls (Fig. 1a). Decreases in BW gain were observed in both vector-treated cohorts, with absolute BW 5–6% lower than the controls, from D1 to 24 weeks pi, though BW differences were not significant among the vector-treated mice and nontreated controls after 6 weeks pi.

No significant differences were observed in food consumption among the rAAV9-treated and nontreated control cohorts.

Vector treatment-related transient increases in blood AST and ALT at 6 weeks pi. Blood chemistry analyses were performed at 6 weeks, 12 weeks, and 24 weeks pi to assess the potential toxicity of systemic rAAV9-CMV-h*NAGLU* gene delivery. Test article-related increases in mean AST and ALT were noted in males of both low-dose (1×10^{14} vg/kg) and high dose (2×10^{14} vg/kg) groups at 6 weeks, 12 weeks, and 24 weeks pi (Fig. 1b and c), in comparison to nontreated controls (Saline). Increases in AST and ALT were also observed at 6 weeks and 24 weeks pi in females treated at the high vector dose (Fig. 1b and c). However, in general, the blood ALT and AST levels in rAAV9-treated mice were close to or within the historical normal ranges (Fig. 1b and c), except ALT in males at 6 weeks pi, indicating that the rAAV9 treatment mediated acute but not persistent liver toxicity at a very high vector dose.

The vector treatments did not lead to detectable changes in other tested blood chemistry parameters. In addition, significant increases in blood lymphocytes were detected only at 6 weeks pi in male mice of the high dose group (Fig. 1d), and no other hematology changes were observed.

Minimal microscopic changes in the liver and heart of rAAV9-treated mice. Tissue samples were examined for histopathological changes to assess toxicity of systemically delivered rAAV9-CMV-h*NAGLU* vector via systemic delivery.

In the liver, vector dose-dependent minimal microscopic changes were observed mostly in male mice, as well as some female animals, at 4 weeks, 12 weeks, and 22 weeks pi (Supplementary Table S2). These changes included minimal single cell hepatocyte necrosis, and increases in hepatocyte mitosis and hepatocyte mineralization. No detectable monocyte infiltration was observed in the liver, and no correlation was observed between serum ALT/AST and hematology (Fig. 1b and c) in rAAV9 treated mice, suggesting minimal involvement of inflammation.

In the heart, minimal to mild cardiomyopathies were observed in both rAAV-treated cohorts, mostly

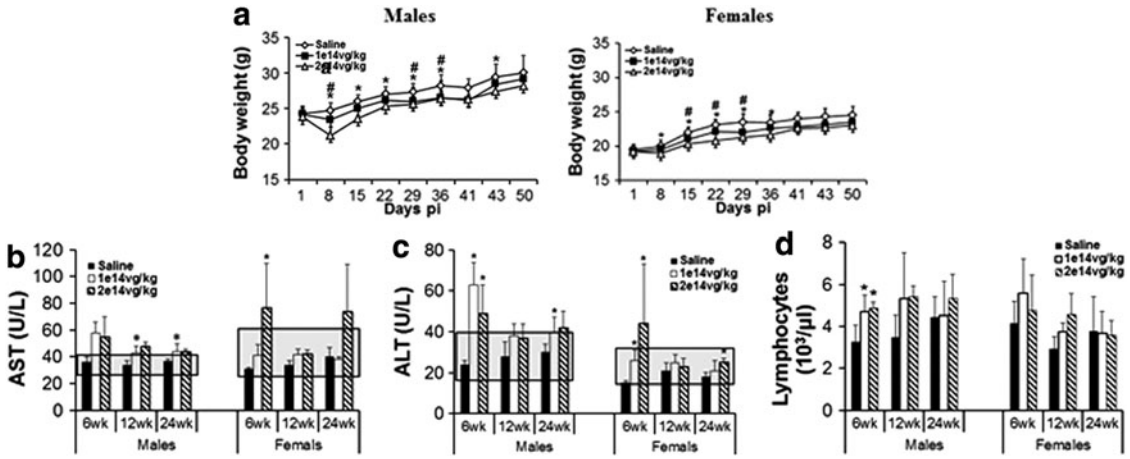

Figure 1. Acute impact of systemic rAAV9-hNAGLU gene delivery on body weights, blood liver enzyme levels, and lymphocytes in mice. WT C57BL/6 mice (8 weeks old) were treated with an IV injection of 1×10^{14} vg/kg or 2×10^{14} vg/kg rAAV9-CMV-h*NAGLU* vector ($N=30$/group, M:F=1:1). **(a)** Body weights (BD) were measured weekly from day 1 through 24 weeks pi. Data are means ± SD. $^{\#}P\leq0.05$ 1×10^{14} vg/kg cohort vs. saline controls; $^{*}P\leq0.05$ 2×10^{14} vg/kg vs. saline controls; **no significant differences in BD between rAAV9-treated and saline control cohorts after 6 weeks pi. Blood was assayed for clinical chemistry and hematology at 6 weeks, 12 weeks, and 24 weeks pi. **(b, c)** Blood AST and ALT levels and **(d)** blood lymphocyte counts. $^{*}P<0.05$ vs. saline controls ($n=3$–5/group); gray shades: historical normal range.

in females, as well as some males, throughout the 24 weeks study duration, without apparent vector dose-association (Supplementary Table S2). Minimal monocyte infiltration was only observed at 24 weeks pi in the low dose cohort, most of which had no detectable cardiomyopathy (Supplementary Table S2), suggesting that inflammation was not the cause of observed cardiomyopathy.

Histopathological examination showed no vector-treatment-related changes in other organs of major systems, including brain, spinal cord, intestines (jejunum, colon), stomach, kidney, spleen, lung, pancreas, lymph node (inguinal), testis, and ovary. The results further support the safety of IV injection of rAAV9-CMV-h*NAGLU* vector as a potential strategy for gene therapy in human patients.

Systemically delivered rAAV9-h*NAGLU* vector-mediated global CNS and broad differential somatic rNAGLU expression following a systemic vector delivery. Brain, spinal cord, and multiple somatic tissues were analyzed at 6 weeks, 12 weeks, and/or 24 weeks pi for NAGLU enzymatic activity and/or immunofluorescence (IF) for hNAGLU to determine the level and distribution of rAAV9-mediated transgene expression.

We observed significant increases in NAGLU enzymatic activity above normal levels in the brain, spinal cord, and multiple somatic tissues in rAAV9-treated subjects compared to nontreated controls (Fig. 2). This suggested effective transduction in both the CNS and somatic system mediated by the systemically delivered rAAV9 vector. Dose responses were observed in brain, spinal cord, heart, pancreas, and lung, but not in kidney, spleen, stomach, and intestine (Fig. 2a and b). The NAGLU activity peaked in all tested somatic tissues at 6 weeks pi and in the CNS at 12 weeks pi (Fig. 2c). The NAGLU activity persisted in the majority of tested tissues (except liver) between 12 weeks and 24 weeks pi (Fig. 2c and d), supporting the long-term transgene expression in the CNS and periphery. Interestingly, liver NAGLU activity in 2×10^{14} vg/kg cohort was reduced to WT levels at 12 weeks and 24 weeks pi, and was much lower than the 1×10^{14} vg/kg cohort (Fig. 2), suggesting potential mechanisms for silencing NAGLU overexpression in the liver, which may be linked to the observed acute liver toxicity in male mice of the high-dose cohort. Notably, higher levels of NAGLU activity were observed in the spinal cord and heart than in the brain and other tissues, especially in the high-dose cohort, though the mechanisms are unclear.

Tissues collected at 24 weeks pi were assayed by IF staining for hNAGLU to visualize the levels and persistence of rAAV9-mediated transgene expres-

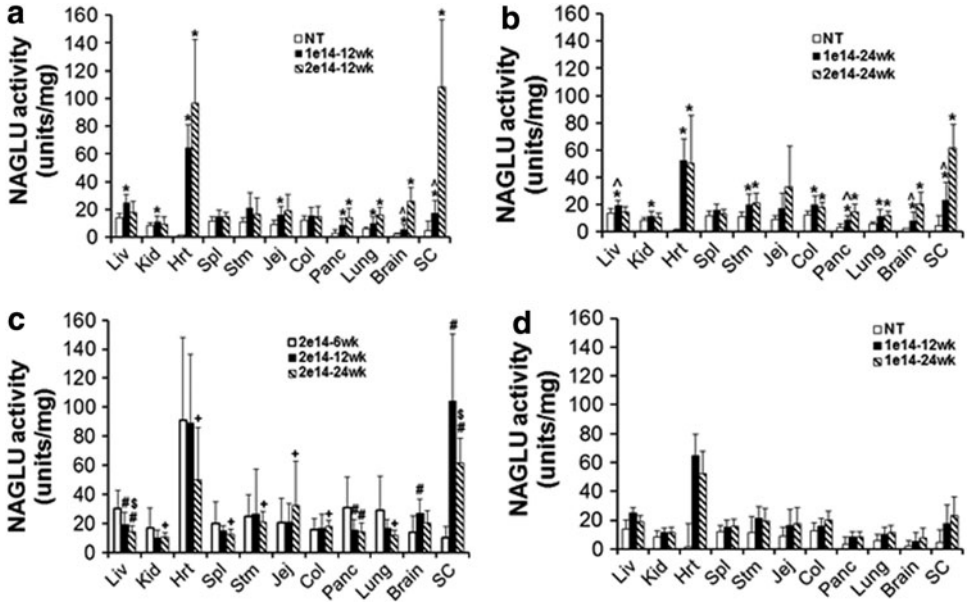

Figure 2. rAAV9-mediated long-term expression of rNAGLU in the CNS and somatic tissues in C57BL/6 mice. WT C57BL/6 mice (8 weeks old) were treated with an IV injection of 1×10^{14} vg/kg or 2×10^{14} vg/kg rAAV9-CMV-h*NAGLU* vector ($N=30$/group, M:F=1:1). Tissues were assayed for NAGLU activity at 6 weeks, 12 weeks, and 24 weeks pi (n=8–10/group). **(a, b)** Dose response comparison of tissue NAGLU activity levels at 12 weeks **(a)** and 24 weeks pi. $^{*}P\leq0.05$ vs. group 1; $^{\wedge}P>0.05$ vs. saline controls. **(c)** Temporal comparison of tissue NAGLU activity levels in mice treated with 2×10^{14} vg/kg rAAV9. $^{*}P\leq0.05$ vs. 6 weeks pi; $^{+}P>0.05$ vs. 6 weeks pi; $^{\$}P>0.05$ vs. 12 weeks pi. **(d)** Temporal comparison of tissue NAGLU activity in mice treated with 1×10^{14} vg/kg rAAV9. NAGLU activity is expressed as units/mg protein; 1 unit=nmol 4-methylumbelliferone (4MU) released per hour. Data are means ± SD.

sion. The results showed overexpression of rNAGLU throughout the CNS (Fig. 3a) in neurons, glia, and endothelial cells in all rAAV9-h*NAGLU* treated mice. The rAAV9-mediated rNAGLU expression was also detected broadly in somatic tissues, including liver, heart, intestine, lung, and pancreas (Fig. 3b), as well as spleen, ovary, and testis (Supplementary Fig. S1). Importantly, IF showed low levels of rNAGLU staining was mostly in endothelial cells, as well as sporadic hepatocytes in the liver of mice treated at 1×10^{14} vg/kg, but completely diminished in mice of the high-dose cohort, correlating to liver NAGLU activity levels (Fig. 2). In the heart, rNAGLU-positive cells were cardiomyocytes and vascular endothelial cells. In the gastrointestinal tract, strong IF rNAGLU signals were detected predominantly in neurons of myoenteric and submucosal plexus (Fig. 3b), suggesting efficient PNS targeting. In lungs, IF staining showed rNAGLU in cuboidal cells and small cells of alveolus (Fig. 3b). We also observed rNAGLU overexpression in the pancreas, in islets cells and acinar cells (Fig. 3b), indicating rAAV9-targeting of both endocrine and exocrine pancreas. In the spleen, rNAGLU signals were detected almost exclusively in sinuosoids in red pulp (Supplementary Fig. S2). Importantly, in the vector treated animals, rNAGLU was observed only in cells beyond follicles in ovary, and only in cells in stroma, but not in seminiferous tubules, in testis (Supplementary Fig. S2), suggesting minimal possibility of vertical transmission. In general, the rNAGLU-positive signals appeared to be localized in granules, supporting lysosomal targeting of rNAGLU (Fig. 3, Supplementary Fig. S2).

Acute antibody responses to AAV9 and rNAGLU had no detectable impact on tissue rNAGLU activity

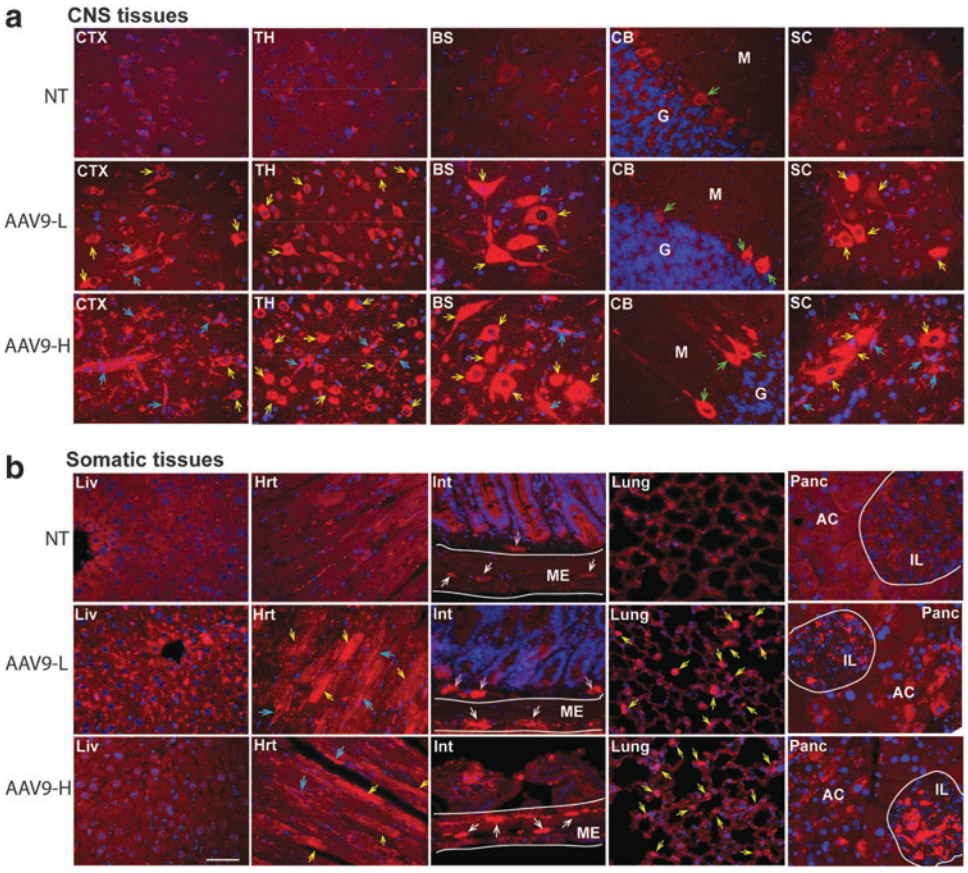

Figure 3. Distribution of AAV9-mediated persistent rNAGLU expression in the CNS and somatic tissues in C57BL/6 mice. WT C57BL/6 mice (8 weeks old) were treated with an IV injection of rAAV9-CMV-h*NAGLU* vector. Tissues were assayed by immunofluorescence (IF) for hNAGLU at 24 weeks pi. Red fluorescence: rNAGLU-positive cells and signals; blue fluorescence: DAPI-positive nuclei. NT, nontreated saline controls; AAV9-L, vector-treated at 1×10^{14} vg/kg; AAV9-H, vector-treated at 2×10^{14} vg/kg. **(a)** CNS tissues: CTX, cerebral cortex; TH, thalamus; BS, brain stem; CB, cerebellum; SC, spinal cord; yellow arrows, rNAGLU-positive neurons; green arrows, Purkinje cells; blue arrows, rNAGLU-positive blood vessels. **(b)** Somatic tissues: Liv, liver; Hrt, heart; yellow arrows, cardiomyocytes; blue arrows, blood vessels; lung, yellow arrows, rNAGLU-positive cells; Int, small intestine; ME, muscularis externa; white arrows, neurons myenteric plexus; pink arrows, neurons of submucosal plexus; panc, pancreas; IL, islets of Langerhans; AC, acinus. Scale bar: 50 μm.

Table 1. *Antibody responses against rAAV9 and rNAGLU in WT C57BL/6 mice following an IV injection of rAAV9-CMV-hNAGLU*

	Anti-AAV9 IgG				*Anti-hNAGLU IgG*			
	1×10^{14} vg/kg		*2×10^{14} vg/kg*		*1×10^{14} vg/kg*		*2×10^{14} vg/kg*	
Time point (pi)	*M*	*F*	*M*	*F*	*M*	*F*	*M*	*F*
6 weeks	1:1,6000	1:51,200	1:51,200	1:51,200	1:400	1:400	1:400	1:400
12 weeks	1:25,600	1:25,600	1:51,200	1:51,200	1:1,600	1:1,600	1:800	1:1,600
24 weeks	1:51,200	1:25,600	1:12,800	1:51,200	1:4,800	1:50	1:400	1:1,600

WT C57BL/6 mice were treated with an IV injection of 2×10^{14} vg/kg rAAV9-CMV-h*NAGLU*. Serum samples were assayed by binding ELISA for IgG against AAV9 and hNAGLU at 6, 12, and 24 weeks pi. The antibody titers are means ($n=3$–5). Anti-AAV9 IgG titers were <1:100 in saline-treated control mice ($n=5$/group).

levels. Serum samples were assayed by binding ELISA for IgG against AAV9 capsid and hNAGLU proteins to assess the vector treatment-induced Ab responses to AAV9 vector and the transgene product. The results showed robust anti-AAV9 Abs in all vector-treated subjects, which peaked at 6 weeks pi and persisted through to the endpoint (24 weeks pi), without significant dose correlation (Table 1). The induced AAV9 Ab responses had no detectable impact on tissue NAGLU activity levels (Fig. 2).

We also detected IgG against hNAGLU in the serum in all rAAV9-treated mice, indicating that the systemic vector delivery induced an Ab response to the transgene product (Table 1). The anti-rNAGLU Ab response appeared to be slower than the anti-AAV9 Ab response, and peaked at 12 weeks pi (Table 1). Importantly, the anti-rNAGLU Abs decreased in the majority of the rAAV9-treated animals after 12 weeks pi (Table 1), suggesting potential tolerance due to the continuous release of secreted rNAGLU in the system, or a lesser immunogenicity. We did not observe a correlation between serum anti-hNAGLU Ab levels (Table 1) and tissue rNAGLU activity (Fig. 2), suggesting that serum anti-hNAGLU Abs have little impact on either the transgene product or rAAV9-transduced cells in tissues.

Systemic rAAV9-hNAGLU gene delivery induced transient T-cell responses to the vector and transgene product. At 6 weeks and 12 weeks pi, splenocytes from the 2×10^{14} vg/kg cohort were assayed by IFN-γ-ELISPOT, in the presence of overlapping synthetic peptide libraries covering full-length AAV9 capsid protein and full-length hNAGLU, to detect T-cell responses against the vector or transgene products in the treated subjects. Positive IFN-γ-forming

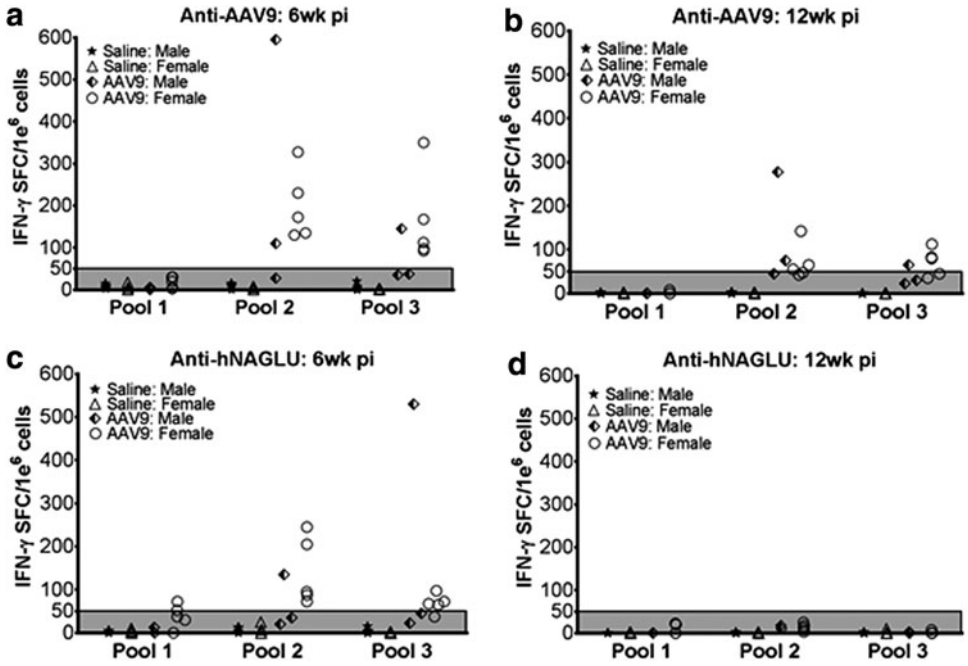

Figure 4. Transient T-cell responses to AAV9 and rNAGLU following systemic rAAV9-hNAGLU administration. WT C57BL/6 mice (8 weeks old) were treated with an IV injection of 2×10^{14} vg/kg rAAV9-CMV-h*NAGLU* vector. Splenocytes were assayed at 6 weeks and 12 weeks pi by IFNγ-ELISpot against overlapping peptides of AAV9-capsid protein **(a, b)** or hNAGLU protein **(c, d)**. Data are from individual subjects, expressed as IFN-γ SFC/1e^6 cells. IFN-γ SFC/1e^6 cells >50 are considered positive.

spots against AAV9 peptide Pool 2 and 3, but not Pool 1, were detected in 7/8 and 6/8 rAAV9-treated mice respectively at 6 weeks pi, which diminished at 12 weeks pi (Fig. 4a and b). We also detected positive IFN-γ-forming spots against hNAGLU peptide Pools 1, 2, and 3 in 2, 6, and 5 of 8 tested mice, respectively, which completely disappeared by 12 weeks pi (Fig. 4c and d). These data indicate that the detected T-cell responses to the vector and rNAGLU were transient, likely as acute immune responses to the systemic rAAV9-h*NAGLU* gene delivery without persistent impacts on tissue rNAGLU expression.

Differential biodistribution of rAAV9 vector genomes (vg) in tissues. Quantitative real-time PCR was performed to determine the amount of rAAV9-CMV-h*NAGLU* vector entering and persisting in the CNS versus somatic tissues at 6 weeks and/or 24 weeks pi. Table 2 shows the differential biodistribution of the vg in different tissues in animals receiving an IV vector injection vs. nontreated animals. At 6 weeks pi, the highest vg concentration was detected in the liver, followed by lung, lymph node, heart, kidney, stomach, pancreas, spleen, ovary, testis, and the CNS tissues (Table 2). Notably, from 6 weeks to 24 weeks pi, vg decreased approximately 16-fold in the liver, but by only 2/3 in the brain of mice in the 2×10^{14} vg/kg dose cohort (Table 2). At 24 weeks pi, no difference was observed in vg in the liver between the low-dose and high-dose cohorts, while there was a perfect two-fold dose-dependent difference in biodistribution in the brain (Table 2). However, there was no correlation between the quantity of tissue vg (Table 2) and rNAGLU expression levels (Fig. 2). While having the same amount of vg at 24 weeks pi (Table 2), the liver NAGLU activity levels in the high-dose cohort were reduced to WT levels and were significantly lower than the low-dose group (Fig. 2), suggesting potential silencing of NAGLU overexpression in WT mouse liver at higher levels of the enzyme.

Table 2. *Biodistribution of rAAV9-CMV-hNAGLU in wild-type C57BL/6 mice*

	10^5 vg/μg DNA		
	Group 3 (2×10^{14} vg/kg)		Group 2 (1×10^{14} vg/kg)
Tissues	*(6 weeks pi)*[a]	*(24 weeks pi)*[b]	*(24 weeks pi)*[c]
Liver	320.118 ± 327.119	20.218 ± 12.597	19.702 ± 8.237[d]
Kidney	11.620 ± 7.122		
Spleen	5.279 ± 2.433		
Heart	11.789 ± 5.092		
Lung	19.764 ± 9.751		
Pancreas	6.626 ± 3.534		
Stomach	7.325 ± 4.855		
Colon	1.752 ± 1.344		
Lymph node	14.498 ± 11.318		
Brain	1.269 ± 1.266	0.394 ± 0.156	0.199 ± 0.132[e]
Spinal cord	1.314 ± 1.139		
Ovary	3.062 ± 2.002		
Testis	1.891 ± 1.967		
Blood	5.242 ± 5.149		

Tissues were assayed by qPCR for rAAV9.CMV.h*NAGLU* vector genome. The vg values are means ± SD (n=8–10/group).

[a]qPCR assays were performed by CRL.

[b]qPCR assays were performed by the corresponding author's lab.

[c]No detectable vector genome in tissues from Group 1 saline control mice ($<0.001\times10^5$ vg/μl DNA).

[d]$P>0.05$ vs. Group 3.

[e]$P=0.05$ vs. Group 3

Supporting 6 weeks non-GLP study in MPS IIIB and WT mice mirroring the GLP-toxicology study: The acute liver toxicity observed in the GLP testing is dose-dependent, sex-linked, and genotype-specific

In response to the acute toxicity observed in the GLP study above, we performed a 6-week, non-GLP toxicology study in MPS IIIB mice and their WT littermates, all males, to further investigate its nature and cause. We treated MPS IIIB mice (10–20 weeks old) and their WT littermates (4–7 weeks old)(n=8/group) with an IV injection of 2×10^{14} vg/kg rAAV9-CMV-h*NAGLU* vector from the same manufacturing lot used in the GLP study. Necropsies were performed for blood and tissue analyses at D5 and 6 weeks pi (n=4/group). Notably, tissue analyses on D5 were critical because tissues from the mice that died of acute toxicity in the GLP study above were post-mortem and were of limited value for analyses.

No detectable adverse events in male MPS IIIB and WT mice during 6 weeks observation following an IV injection of 2×10^{14} vg/kg rAAV9-CMV-h*NAGLU*. We did not observe mortality or detectable adverse events in either the rAAV9-treated WT or MPS IIIB mice during the duration of the 6-week experiments.

At necropsy on D5 pi, pale liver color was seen in one of the rAAV9-treated wt mice. Because all five animals with acute mortality in our GLP tox study had similar liver pallor, we believe that this animal would likely have died on D6–8 pi if it had not been terminated. No abnormal tissue appearance was observed in other animals necropsied on D5 pi, including 3 WT mice and 4 MPS IIIB mice treated with 2×10^{14} vg/kg vector. No abnormal tissue appearance was observed in either WT or MPS IIIB mice necropsied at 6 weeks pi (n=4/group).

No significant changes in blood chemistry in rAAV9-treated MPS IIIB mice during the 6-week observation. Blood samples (n=3-4/group) were collected at the time of necropsies and assayed for

selected blood chemistry parameters, including alanine aminotransferase (ALT), aspartate aminotransferase (AST), creatine phosphokinase (CPK), alkaline phosphatase (ALP), gamma-glutamyl transferase (GGT), creatinine (CREAT), blood urea nitrogen (BUN), triglycerides TRIG, total bilirubin (TBIL), and total serum protein (TSP). Unfortunately, the blood samples from four WT mice on D5 pi were accidently lost.

No abnormal changes were detected in any of the tested blood parameters in MPS IIIB mice at D5 pi (Supplementary Table S3), suggesting that the observed acute mortality in our GLP study is likely genotype-specific. At 6 weeks pi, while elevated liver enzymes (AST and ALT) were limited to rAAV9-treated WT mice (2–3/4), the muscle enzyme (CPK) was increased in both rAAV9-treated WT (2/4) and MPS IIIB mice (2/4), although the magnitude of the effect was substantially higher in the WT animals (Supplementary Table S3). However, because increases in ALT, AST, and CPK were also observed in nontreated WT control mice, the changes in rAAV9-treated MPS IIIB mice may not be significant.

Differential biodistribution of rAAV9-CMV-h*NAGLU* vector. Using qPCR, we detected differential distribution of the rAAV9-CMV-h*NAGLU* genome in the CNS and peripheral tissues at D5 and 6 weeks pi (Fig. 5). Significant decreases in vector genome were observed in virtually all tested tissues in both the AAV9-treated wt and MPS IIIB mice from D5 to 6 weeks pi (Fig. 5), though the mechanisms are unclear. There were no significant differences in vg levels in kidney, intestine, lung, and skeletal muscle between the rAAV9-treated WT and MPS IIIB mice at either time point (Fig. 5). Significantly higher vg levels were detected in liver, brain, heart, and spleen in MPS IIIB mice compared to those in WT mice at both D5 and 6 weeks pi, while at 6 weeks pi there were more vg in muscles in WT than MPS IIIB mice (Fig. 5), suggesting that disease pathology may affect the transduction efficiency in these tissues.

Rapid effective transgene expression in the CNS and somatic tissues following an IV rAAV9-h*NAGLU* vector delivery. Tissues were assayed for NAGLU activity and IF at D5 and 6 weeks after an IV injection of rAAV9-CMV-h*NAGLU* vector to assess the transgene expression.

Supranormal levels of NAGLU activity were detected in all tested tissues in both WT and MPS IIIB mice receiving the vector (Fig. 6) as early as D5 pi, indicating rapid efficient CNS and somatic transduction. The NAGLU activity levels peaked at D5 pi in the majority of tested tissues in both WT and MPS IIIB mice, with the exception of heart and brain in MPS IIIB mice, and muscle and brain in WT mice (Fig. 6). Between D5 and 6 weeks pi, NAGLU activity levels persisted or increased in the majority of

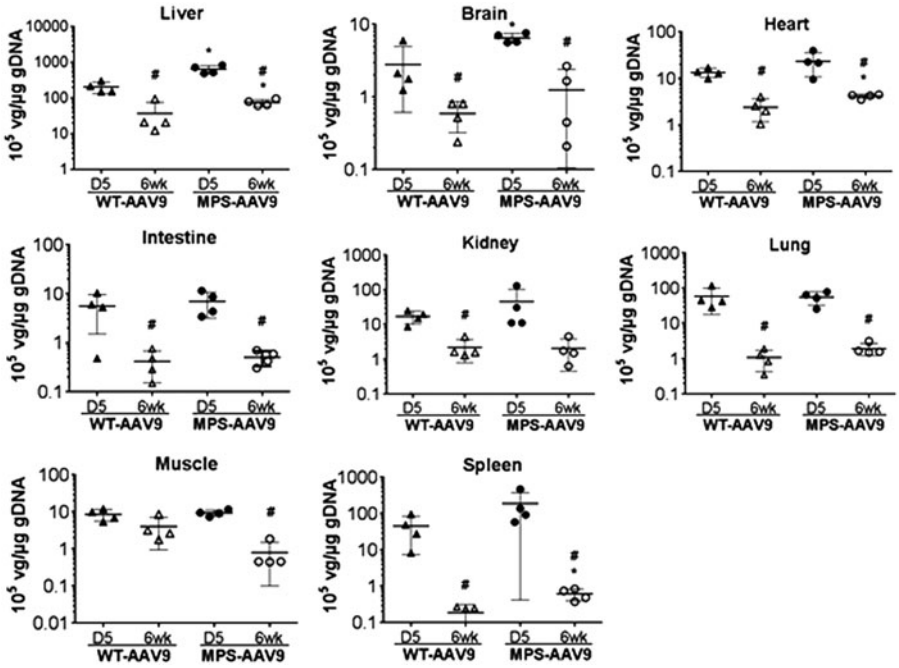

Figure 5. Biodistribution of rAAV9-hNAGLU vector in MPS IIIB and WT mice following a systemic delivery. MPS IIIB mice and their WT littermates, all males, were treated with an IV injection of 2×10^{14} vg/kg rAAV9-CMV-h*NAGLU*. Tissues were assayed by qPCR at D5 and 6 weeks pi for vector genome (n = 4/group). Data are means ± SD, expressed as 10^5 vg/μg genomic DNA. *No detectable vector genome in tissues from nontreated control animal mice (<0.001×10^5 vg/μg gDNA).

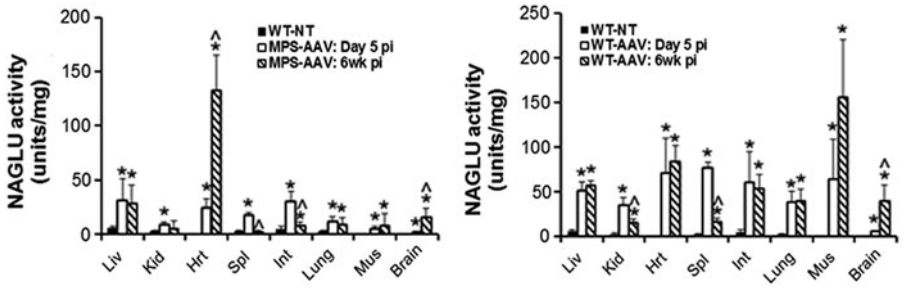

Figure 6. rAAV9-mediated rapid rNAGLU expression in the CNS and somatic tissues in MPS IIIB and WT mice. MPS IIIB mice and their WT littermates, all males, were treated with an IV injection of 2×10^{14} vg/kg rAAV9-CMV-h*NAGLU*. Tissues were assayed for NAGLU activity at D5 and 6 weeks pi (n = 4/group). WT-NT, nontreated WT mice; MPS-AAV, rAAV9-treated MPS IIIB mice; WT-AAV, rAAV9-treated WT mice. NAGLU activity is expressed as units/mg protein; 1 unit = nmol 4MU released per hour. Data are means ± SD. $*P \le 0.05$ vs. nontreated WT mice; $\wedge P \le 0.05$ 6 weeks vs. D5 pi.

the tissues in both WT and MPS IIIB mice, except in the spleen, with a significant reduction in NAGLU activity, suggesting a potential acute innate immune response to the vector. In general, higher NAGLU activity levels were detected in all tested tissues in rAAV9-treated WT mice, compared to MPS IIIB mice, except in the heart at 6 weeks pi (Fig. 6). It is worth noting that there was endogenous NAGLU activity in WT mice (Fig. 6), but no detectable NAGLU activity in any tissues in nontreated MPS IIIB mice. No clear correlation was observed between NAGLU activity levels (Fig. 6) and tissue vector genome levels (Fig. 5). The NAGLU expression pattern differences in heart and muscle between wt and MPS IIIB mice (Fig. 6) suggests potential impact of genotypes or, more specifically, disease pathology on the transduction efficiency.

Tissues were also assayed by IF for hNAGLU to visualize the transgene expression. Our data showed rNAGLU throughout the CNS and in widespread somatic tissues in both rAAV9-treated WT and MPS IIIB mice at both D5 and 6 weeks pi, indicating rapid and persistent transgene expression, though with clear differences in the liver between WT and MPS IIIB mice (Fig. 7, Supplementary Fig. S3). At D5 pi, we observed diffuse NAGLU expression in the liver in hepatocytes and endothelial cells of capillaries and larger blood vessels in MPS IIIB mice (Fig.7a). Importantly, highly hNAGLU-expressing hepatocytes that lacked nuclei were observed in three of four rAAV9-treated WT mice, indicating hepatic necrosis. Notably, the highly rNAGLU-positive and nuclear-deficient hepatocytes were observed in approximately 30% of hepatocytes in the mouse that had discolored liver at necropsy, while involving only sporadic single cells (<2%) in two other WT mice (Fig. 7a).

Further, in general, liver rNAGLU signals appeared to be predominantly in endothelial cells of vasculature in WT mice with reduced intensity at 6 weeks pi, while persistent in abundant hepatocytes and endothelial cells in MPS IIIB mice (Fig.7b). No necrotic NAGLU-positive hepatocytes were observed in rAAV9-treated MPS IIIB mice (Fig.7), suggesting that the observed acute liver toxicity is likely genotype-specific. In spleen, rNAGLU was detected in endothelial cells of sinusoid in red pulp (Supplementary Fig. S3). In lungs, rNAGLU was detected in large cuboidal cells in alveoli, possibly type II pneumocytes (Supplementary Fig. S3). In the intestine, the rNAGLU-positive cells were predominantly neurons in myenteric and submucosal plexus (Supplementary Fig. S3). Importantly, in the eyes, we observed rNAGLU in the ciliary processes, in ganglion cells, and in cells of the inner nuclear layer (INL) in the retina, suggesting optic nervous system targeting (Supplementary Fig. S3). Our data also showed rNAGLU in the pancreas, in cells in islets and acini, indicating transduction of both endocrine and exocrine pancreatic tissues (Supplementary Fig. S3). Strong rNAGLU IF staining was seen in >50% adipocytes in fat tissues (Supplementary Fig. S3). Further, IF showed rNAGLU in abundant endothelial cells of vasculatures in virtually all tested tissues, but could not be presented well in many images due to poor contrast with the background signals. These data further indicate the broad tissue tropism and clinical relevance of systemic rAAV9-h*NAGLU* gene delivery.

Histopathology assessments. Histopathology examinations were performed on brain and multiple somatic tissues from all rAAV9-treated wt and MPS IIIB mice on D5 pi and 6 weeks pi (n = 4/group), controls were nontreated wt and MPS IIIB mice. At D5 pi, there was minimal to mild hepatic necrosis noted in the majority of rAAV9-treated WT mice and moderate hepatic necrosis in the WT mice that had pale liver at necropsy (Supplementary Fig. S4). No hepatic necrosis was observed in WT mice at 6 weeks pi or in MPS IIIB mice at either

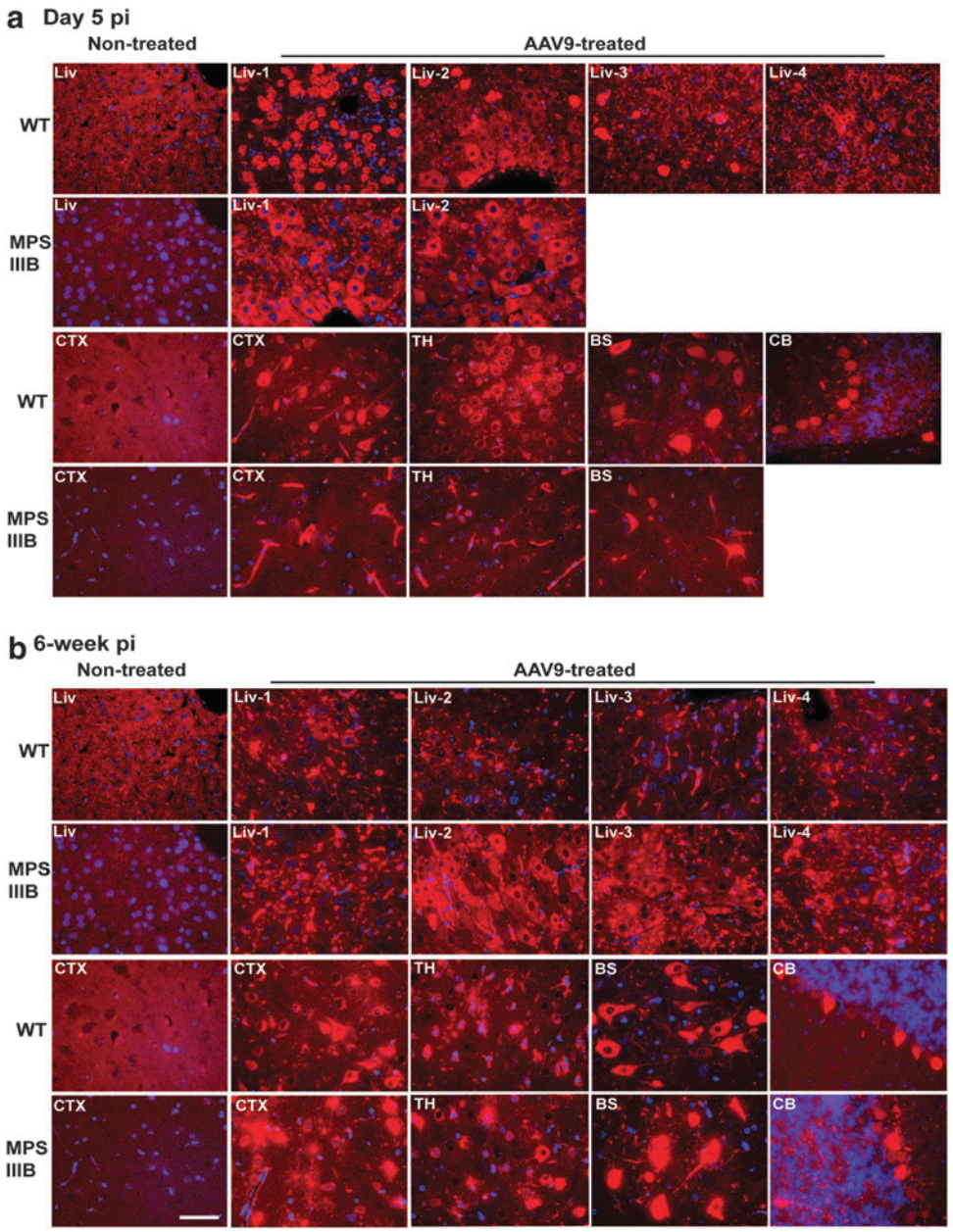

Figure 7. Comparison of AAV9-mediated rNAGLU expression in MPS IIIB and WT mice after an IV rAAV9-hNAGLU gene delivery. MPS IIIB mice and their WT littermates, all males, were treated with an IV injection of 2×10^{14} vg/kg rAAV9-CMV-h*NAGLU*. Tissues were assayed by IF for hNAGLU at D5 **(a)** and 6 weeks pi **(b)**. Red fluorescence, rNAGLU-positive cells and signals; blue fluorescence, DAPI-positive nuclei; Liv 1–4, liver samples from individual subjects; CTX, cerebral cortex; TH, thalamus; BS, brain stem; CB, cerebellum; G, granule layer; M, molecular layer. Scale bar: 50μm.

D5 (Supplementary Fig. S4) or 6 weeks pi. Importantly, liver morphology in rAAV9-treated MPS IIIB mice appeared to be normal, while fine cytoplasmic vacuoles, consistent with lysosomal storage, were observed in the livers of all non-treated MPS IIIB control mice (Supplementary Fig. S4), indicating the rapid effective functional impact of rNAGLU on clearance of lysosomal GAG storage.

In rAAV9-treated MPS IIIB mice, minimal or mild focal necrosis of cardiac myofibers was noted at 6 weeks, but not at D5 pi. This change was not detected in the vector-treated WT mice, two of which displayed abnormal higher levels of serum CPK. Notably, much higher levels of NAGLU activity was observed in the hearts of rAAV9-treated MPS IIIB mice than in rAAV9-treated WT mice at 6 weeks pi (Fig. 6), suggesting a potential link between the observed cardiomyopathy and rNAGLU overexpression. No other abnormal histopathological changes were noted in any of the tested tissues.

DISCUSSION

As previously reported, we have developed an effective gene therapy approach for treating both the neurological and somatic disorders of MPS IIIB by a single IV delivery of rAAV9-CMV-h*NAGLU* vector.[22,45] Our previous study showed a safe and translatable profile for this approach in nonhuman primates (NHP) at the designated minimal efficacious clinical dose, 2×10^{13} vg/kg.[42]

To prepare for a phase 1/2 clinical trial in MPS IIIB patients, we performed this GLP-compliant toxicology/biodistribution study to test the rAAV9-CMV-h*NAGLU* vector at doses two- and four-fold higher than our proposed clinical high dose (5×10^{13} vg/kg), following FDA guidelines. The most important finding of this study is the dose-limiting, sex-associated, and genotype-specific severe acute liver toxicity in 1/3 of WT male mice at D6–8 pi following an IV injection of the vector at 2×10^{14} vg/kg, leading to severe hepatocyte necrosis and mortality. This acute liver toxicity was linked to rNAGLU overexpression in hepatocytes in male WT mice but not female WT mice, MPS IIIB mice receiving the same vector dose, or WT mice treated with the vector at a dose two-fold lower (1×10^{14} vg/kg). The possibility of inflammatory involvement in this acute liver toxicity is unlikely, given the absence of detectable cellular infiltration in the liver. We believe that we may have identified the upper dosing limit of rAAV9-CMV-h*NAGLU* via a systemic delivery. It is likely that 2×10^{14} vg/kg is close to the safe dosing threshold, and the severe acute liver toxicity observed in WT mice might also occur in MPS IIIB mice if higher doses were used. Further, this study suggests that there might be a limit for transgene expression levels in the liver, and that over-the-limit transgene expression may not be feasible for clinical application due to the potential severe toxicity.

Despite the acute hepatic toxicity observed in 1/3 of male WT mice treated with a high vector dose, we demonstrate here a largely safe profile of systemic rAAV9-CMV-h*NAGLU* gene delivery. The possibilities of chronic toxicity and other acute damages were minimal in both WT and MPS IIIB mice that received an IV injection of the rAAV9-h*NAGLU* vector at 1×10^{14} vg/kg and 2×10^{14} vg/kg, which are two-fold and four-fold higher than the proposed high dose (5×10^{13} vg/kg) for our planned phase 1/2 gene therapy clinical trial in MPS IIIB patients.

This GLP-toxicology study further confirmed the broad tissue tropism of rAAV9, similar to previously reported.[22] More importantly, using exceptionally high vector doses and better tissue availability enabled the demonstration of expanded clinical relevance and potential of rAAV9 for treating the neurological and broad somatic diseases, which were not visible when using lower doses. We demonstrate a rapid emergence of rAAV9-mediated transgene expression that peaked in the majority of tissues before 5 days pi and persisted in both WT and MPS IIIB mice. An important finding is rNAGLU expression in broad cell types in the eye, including neuronal and non-neuronal cells in retina and cells of ciliary processes, supporting the potential for optic nervous system targeting and expanded neurological benefits. This is particularly important, given that ocular manifestations, especially retinonopathy, are common among MPS III patients.[46] In addition, the effective transduction in ciliary process, because of their secretory function, may offer significant therapeutic impacts as sources providing the enzyme to broad areas of the eye. Another significant finding is that the systemically delivered rAAV9 transduces both the endocrine and exocrine pancreatic tissues, offering the potential for treating LSDs and pancreatic disorders. In addition, predominant transduction of type II pneumocytes and endothelial cells indicates the potential of AAV9 pulmonary targeting, since type II pneumocytes constitute 60% of alveolar epithelial cells and function to reduce surface tension and as progenitor cells for both type I and II alveolar cells.[47,48]

The risk of germline transmission of vector sequences in humans has been a major safety concern for gene therapy, especially when targeting young subjects. Numerous studies indicate minimal risk of germline transmission for humans when using rAAV2 vector.[49] In this study, an IV-delivered rAAV9-CMV-h*NAGLU* vector led to transgene expression in reproductive organs in both male and female mice, but exclusively in nongermline cells in the ovary and testis, even at a very high dose. Previous studies demonstrated efficient function of the CMV promoter in germline cells in mice, which would have facilitated visualization if there had been significant transduction.[50] Germline transmission of the rAAV9 vector is therefore unlikely in mice, and may pose minimal risk to humans.

Our data demonstrate that the rAAV9-mediated transgene expression after an IV delivery is rapid in all tested tissues, peaking before D5 pi in both WT and/or MPS IIIB mice, except in the brain and spinal cord, which peak between 6 weeks and 12 weeks pi. While similar broad tissue tropisms of rAAV9 transduction were reproduced, in general, NAGLU activity levels were higher in virtually all tested tissues in WT than MPS IIIB mice, which may be attributable to the presence of endogenous NAGLU in WT animals. Importantly, the rAAV9-mediated transgene expression was persistent in

virtually all tested tissues over the 24-week study duration, with the exception of the liver in WT mice that received a very high dose of the vector. Unexpectedly, there was no dose-response in rNAGLU expression in the majority (7/10) of tested tissues at 12–24 weeks pi in rAAV9-treated WT mice, except in the pancreas and the CNS tissues. Whether this is due to an intrinsic limit on how much of the enzyme can be expressed in some cell types, or saturation in the ability of these cells to take up the vector, is not clear.

Interestingly, at 24 weeks pi, the liver NAGLU activity was at supranatural levels in WT mice treated with the low dose of vector, but reduced to endogenous levels in WT mice receiving the high dose, though both dose cohorts had the same number of vg in the liver. These data strongly suggest some degree of self-regulation of NAGLU expression levels, possibly through promoter silencing when toxic levels have been reached. Why we do not see this effect in the MPS IIIB mice is not clear. However, these cells are lacking of NAGLU, and the rNAGLU expression might never reach toxic levels. Alternatively, the disease pathology may have an impact on the rAAV9 transduction efficiency or tropism, given that rNAGLU levels were significantly higher in heart and lower in muscle in MPS IIIB mice than in WT. In this case, the expression levels correlate with the significantly higher vg in heart and less in muscle in MPS IIIB vs. WT mice, suggesting that the disease pathology may have changed the susceptibility of the cells to AAV9 infection in these tissues. The cardiomyopathy observed in some rAAV9-treated WT and MPS IIIB mice in this study may also be attributable to rNAGLU overexpression in the heart. However, cardiomyopathy was not observed in previous studies in MPS IIIB mice and NHP that were treated with the same rAAV9-h*NAGLU* vector at lower doses (5×10^{12}–2×10^{13} vg/kg),[22,42] suggesting that there is a safe range for NAGLU expression in the heart.

Notably, there are no correlations but are great disparities between tissue rNAGLU expression and vg levels, or vector doses in AAV9-treated WT mice. This study also showed a rapid and continuous loss of vg in all tested CNS and peripheral tissues in mice, even though rNAGLU expression levels were stabilized in the majority of tissues at 6 weeks or 12 weeks pi. Therefore, there might be more biophysiological regulation mechanisms in tissues to maintain NAGLU expression at relatively safe levels, in addition to silencing.

In summary, this GLP-toxicology study delineates a dosing range in which generally safe and effective rAAV9-CMV-h*NAGLU* systemic gene delivery can be utilized for the treatment of MPS IIIB.

ACKNOWLEDGMENTS

We would like to thank Ms. Robyn Cunningham for quality assurance evaluation of the GLP-testing facilities. This study was sponsored by a translational research grant from NIH/NINDS (U01 NS069626). The Drug and Devices Development Service at NCH was supported by a CTSA grant from NIH (UL1TR001070). The Comparative Pathology and Mouse Phenotyping Shared Resource, Department of Veterinary Biosciences and the Comprehensive Cancer Center, at OSU, is supported in part by a grant from NIH/NCI (P30 CA016058).

AUTHOR DISCLOSURE

Fu and McCarty hold stock in Abeona Therapeutics Inc. All other coauthors have no competing financial interests.

REFERENCES

1. Neufeld EF, Muenzer J. The mucopolysaccharidoses. In: The metabolic & molecular basis of inherited disease, 8th ed. CR Scriver, AL Beaudet, WS Sly, and D Valle, eds. McGraw-Hill, New York, St Louis, San Francisco. 2001; pp. 3421–3452.
2. Ryazantsev S, Yu WH, Zhao HZ, Neufeld EF, Ohmi K. Lysosomal accumulation of SCMAS (subunit c of mitochondrial ATP synthase) in neurons of the mouse model of mucopolysaccharidosis III B. Mol Genet Metab 2007;90:393–401.
3. Ohmi K, Greenberg DS, Rajavel KS, et al. Activated microglia in cortex of mouse models of mucopolysaccharidoses I and IIIB. Proc Natl Acad Sci U S A 2003;100:1902–1907.
4. Ohmi K, Kudo LC, Ryazantsev S, et al. Sanfilippo syndrome type B, a lysosomal storage disease, is also a tauopathy. Proc Natl Acad Sci U S A 2009;106:8332–8337.
5. McGlynn R, Dobrenis K, and Walkley SU. Differential subcellular localization of cholesterol, gangliosides, and glycosaminoglycans in murine models of mucopolysaccharide storage disorders. J Comp Neurol 2004;480:415–426.
6. Li HH, Yu WH, Rozengurt N, et al. Mouse model of Sanfilippo syndrome type B produced by targeted disruption of the gene encoding alpha-N-acetylglucosaminidase. Proc Natl Acad Sci U S A 1999;96:14505–14510.
7. Li HH, Zhao HZ, Neufeld EF, Cai Y, Gomez-Pinilla F. Attenuated plasticity in neurons and astrocytes in the mouse model of Sanfilippo syndrome type B. J Neurosci Res 2002;69:30–38.
8. DiRosario J, Divers E, Wang C, et al. Innate and adaptive immune activation in the brain of MPS IIIB mouse model. J Neurosci Res 2009;87:978–990.
9. Villani GR, Di Domenico C, Musella A, et al. Mucopolysaccharidosis IIIB: oxidative damage and cytotoxic cell involvement in the neuronal pathogenesis. Brain research 2009;1279:99–108.
10. Villani GR, Gargiulo N, Faraonio R, et al. Cytokines, neurotrophins, and oxidative stress in brain

disease from mucopolysaccharidosis IIIB. J Neurosci Res 2007;85:612–622.

11. Weber B, Guo XH, Kleijer WJ, et al. Sanfilippo type B syndrome (mucopolysaccharidosis III B): allelic heterogeneity corresponds to the wide spectrum of clinical phenotypes. Eur J Hum Genet 1999;7:34–44.
12. Yogalingam G, Weber B, Meehan J, Rogers J, Hopwood JJ. Mucopolysaccharidosis type IIIB: characterisation and expression of wild-type and mutant recombinant alpha-N-acetylglucosaminidase and relationship with sanfilippo phenotype in an attenuated patient. Biochim Biophys Acta 2000; 1502:415–425.
13. Rohrbach M, and Clarke JT. Treatment of lysosomal storage disorders : progress with enzyme replacement therapy. Drugs 2007;67: 2697–2716.
14. Pardridge WM. Drug and gene delivery to the brain: the vascular route. Neuron 2002;36:555–558.
15. Sands MS, and Haskins ME. CNS-directed gene therapy for lysosomal storage diseases. Acta Paediatr Suppl 2008;97:22–27.
16. Berns KI, and Linden RM. The cryptic life style of adeno-associated virus. Bioessays 1995;17:237–245.
17. Daya S, and Berns KI. Gene therapy using adeno-associated virus vectors. Clinical microbiology reviews 2008;21:583–593.
18. Fu H, Kang L, Jennings JS, et al. Significantly increased lifespan and improved behavioral performances by rAAV gene delivery in adult mucopolysaccharidosis IIIB mice. Gene Ther 2007;14: 1065–1077.
19. Fu H, Muenzer J, Samulski RJ, et al. Self-complementary adeno-associated virus serotype 2 vector: global distribution and broad dispersion of AAV-mediated transgene expression in mouse brain. Mol Ther 2003;8:911–917.
20. Fu H, Samulski RJ, McCown TJ, et al. Neurological correction of lysosomal storage in a mucopolysaccharidosis IIIB mouse model by adeno-associated virus-mediated gene delivery. Mol Ther 2002;5:42–49.
21. McCarty DM, DiRosario J, Gulaid K, Muenzer J, and Fu H. Mannitol-facilitated CNS entry of rAAV2 vector significantly delayed the neurological disease progression in MPS IIIB mice. Gene Ther 2009;16:1340–1352.
22. Fu H, Dirosario J, Killedar S, Zaraspe K, and McCarty DM. Correction of Neurological Disease of Mucopolysaccharidosis IIIB in Adult Mice by rAAV9 Trans-Blood-Brain Barrier Gene Delivery. Mol Ther 2011:1025–1033.
23. Desmaris N, Verot L, Puech JP, et al. Prevention of neuropathology in the mouse model of Hurler syndrome. Ann Neurol 2004;56:68–76.
24. Heuer GG, Passini MA, Jiang K, et al. Selective neurodegeneration in murine mucopolysaccharidosis VII is progressive and reversible. Ann Neurol 2002;52:762–770.
25. Liu G, Martins I, Wemmie JA, Chiorini JA, and Davidson BL. Functional correction of CNS phenotypes in a lysosomal storage disease model using adeno-associated virus type 4 vectors. J Neurosci 2005;25:9321–9327.
26. Fraldi A, Hemsley K, Crawley A, et al. Functional correction of CNS lesions in an MPS-IIIA mouse model by intracerebral AAV-mediated delivery of sulfamidase and SUMF1 genes. Hum Mol Genet 2007;16:2693–2702.
27. Heldermon CD, Ohlemiller KK, Herzog ED, et al. Therapeutic efficacy of bone marrow transplant, intracranial AAV-mediated gene therapy, or both in the mouse model of MPS IIIB. Mol Ther 2010;18:873–880.
28. Ruzo A, Garcia M, Ribera A, et al. Liver production of sulfamidase reverses peripheral and ameliorates CNS pathology in mucopolysaccharidosis IIIA mice. Mol Ther 2012;20:254–266.
29. Baek RC, Broekman ML, Leroy SG, et al. AAV-mediated gene delivery in adult GM1-gangliosidosis mice corrects lysosomal storage in CNS and improves survival. PLoS One 2010;5: e13468.
30. Kaplitt MG, Feigin A, Tang C, et al. Safety and tolerability of gene therapy with an adeno-associated virus (AAV) borne GAD gene for Parkinson's disease: an open label, phase I trial. Lancet 2007;369:2097–2105.
31. Worgall S, Sondhi D, Hackett NR, et al. Treatment of late infantile neuronal ceroid lipofuscinosis by CNS administration of a serotype 2 adeno-associated virus expressing CLN2 cDNA. Hum Gene Ther 2008;19:463–474.
32. McPhee SW, Janson CG, Li C, et al. Immune responses to AAV in a phase I study for Canavan disease. J Gene Med 2006;8:577–588.
33. Marks WJ, Jr., Bartus RT, Siffert J, et al. Gene delivery of AAV2-neurturin for Parkinson's disease: a double-blind, randomised, controlled trial. Lancet Neurol 2010;9:1164–1172.
34. Mittermeyer G, Christine CW, Rosenbluth KH, et al. Long-term evaluation of a phase 1 study of AADC gene therapy for Parkinson's disease. Hum Gene Ther 2012;23:377–381.
35. Bartus RT, Baumann TL, Siffert J, et al. Safety/feasibility of targeting the substantia nigra with AAV2-neurturin in Parkinson patients. Neurology 2013;80:1698–1701.
36. Tardieu M, Zerah M, Husson B, et al. Intracerebral administration of adeno-associated viral vector serotype rh.10 carrying human SGSH and SUMF1 cDNAs in children with mucopolysaccharidosis type IIIA disease: results of a phase I/II trial. Hum Gene Ther 2014;25:506–516.
37. Zincarelli C, Soltys S, Rengo G, and Rabinowitz JE. Analysis of AAV serotypes 1–9 mediated gene expression and tropism in mice after systemic injection. Mol Ther 2008;16:1073–1080.
38. Foust KD, Nurre E, Montgomery CL, et al. Intravascular AAV9 preferentially targets neonatal neurons and adult astrocytes. Nat Biotechnol 2009;27:59–65.
39. Duque S, Joussemet B, Riviere C, et al. Intravenous administration of self-complementary AAV9 enables transgene delivery to adult motor neurons. Mol Ther 2009;17:1187–1196.
40. Foust KD, Wang X, McGovern VL, et al. Rescue of the spinal muscular atrophy phenotype in a mouse model by early postnatal delivery of SMN. Nat Biotechnol 2010;28:271–274.
41. Ruzo A, Marco S, Garcia M, et al. Correction of pathological accumulation of glycosaminoglycans in central nervous system and peripheral tissues of MPSIIIA mice through systemic AAV9 gene transfer. Hum Gene Ther 2012;23:1237–1246.
42. Murrey DA, Naughton BJ, Duncan FJ, et al. Feasibility and safety of systemic rAAV9-hNAGLU delivery for treating mucopolysaccharidosis IIIB: toxicology, biodistribution, and immunological assessments in primates. Hum Gene Ther Clin Dev 2014;25:72–84.
43. Mendell JR, Rodino-Klapac LR, Rosales-Quintero X, et al. Limb-girdle muscular dystrophy type 2D gene therapy restores alpha-sarcoglycan and associated proteins. Ann Neurol 2009;66:290–297.
44. Thompson JN, and Nowakowski RW. Enzymatic diagnosis of selected mucopolysaccharidoses: Hunter, Morquio type A, and Sanfilippo types A, B, C, and D, and procedures for measurement of 35SO4-glycosaminoglycans. In: Techniques in Diagnostic Human Biochemical Genetics - A Laboratory Manual. FA Hommes, ed. Wiley-Liss, New York. 1991; pp. 567–586.
45. Naughton BJ, Duncan FJ, Murrey D, et al. Amyloidosis, synucleinopathy, and prion encephalopathy in a neuropathic lysosomal storage disease: the CNS-biomarker potential of peripheral blood. PLoS One 2013;8:e80142.
46. Ashworth JL, Biswas S, Wraith E, and Lloyd IC. Mucopolysaccharidoses and the eye. Surv Ophthalmol 2006;51:1–17.
47. Fehrenbach H. Alveolar epithelial type II cell: defender of the alveolus revisited. Respir Res 2001;2:33–46.
48. Rock JR, and Hogan BL. Epithelial progenitor cells in lung development, maintenance, repair, and disease. Annu Rev Cell Dev Biol 2011;27:493–512.
49. Schuettrumpf J, Liu JH, Couto LB, et al. Inadvertent germline transmission of AAV2 vector: findings in a rabbit model correlate with those in a human clinical trial. Mol Ther 2006;13:1064–1073.
50. Villuendas G, Gutierrez-Adan A, Jimenez A, et al. CMV-driven expression of green fluorescent protein (GFP) in male germ cells of transgenic mice and its effect on fertility. Int J Androl 2001;24:300–305.